Journal of Catalysis 284 (2011) 207–214

Contents lists available at SciVerse ScienceDirect

Journal of Catalysis

journal homepage: www.elsevier.com/locate/jcat

Tuning the activity by controlling the wettability of MOF eggshell catalysts: A quantitative structure–activity study

Sonia Aguado, Jerome Canivet, Yves Schuurman, David Farrusseng *

Institut de Recherches sur la Catalyse et l'Environnement de Lyon (IRCELYON), UMR5256, CNRS/Université Claude Bernard, Lyon 1, 2 Av. A. Einstein, F-69626 Villeurbanne, France

ARTICLE INFO

Article history:
Available online 4 November 2011

Keywords:
Heterogeneous catalysis
Metal-organic frameworks
Hydrophobization
Post-synthetic modification

ABSTRACT

In this work, we report a quantitative structure-activity relationship of functionalized ZIF-type materials (SIM, Substituted Imidazolate Material). Keeping the catalytic center unmodified, post-synthetic modification allows an efficient control of the hydrophilic–hydrophobic balance which drives the competitive adsorption of reactants and products. Hence, we attribute the increase in the reaction rate of Knoevenagel condensation (up to seven times) to the modification of the environment of catalytic sites through the creation of hydrophobic environment surrounding the catalytic sites. Surface tension properties are monitored by measuring the contact angle with a water droplet on a SIM thin film grown on a flat support. We show that the contact angle is directly correlated to the catalytic activity of Knoevenagel condensation. Hence, we propose that the contact angle of a catalyst thin layer with water can be a quantitative descriptor of direct relevance for catalytic processes which produces water and/or for catalysts that are poisoned with water. Finally, we measured the intrinsic reaction rate free of external and internal diffusion limitations by controlling the thickness of the SIM shell on SIM/alumina beads. Insights on the localization of the active sites (surface vs. bulk) are provided.

1. Introduction

Metal-organic frameworks (MOFs) are a new class of hybrid porous materials that are very attractive to design new type of catalysts [1–8]. Their catalytic properties arise from structural features already present on their frameworks such as open metal centers [9–13], acid bridging hydroxyl [14] or accessible N-bases on the organic linkers [15,16]. Because of their well-defined structure and site isolation, MOFs are found to be a very appropriate class of model solid catalysts. Indeed, it is possible in practice to change one particular feature without affecting the others, which is usually a challenge for other porous inorganic catalysts. For example, it is possible to control the pore size by selecting longer ligands, everything else remaining the same. It is also possible, to a certain extent, to synthesize isomorphous structures with different cations; MIL-53 compounds can be obtained by a wide range of metal cations such as Al^{3+}, Ga^{3}, Fe^{3+} or Cr^{3+} others, and eventually mixture of thereof [17]. With the purpose of getting more sophisticated MOF catalysts, post-synthetic modification (PSM) methods have been recently developed [18–20]. It consists in the chemical modification of the solid after formation of the parent crystalline structure by grafting organic or organometallic species onto the parent MOF host without significant modification of the initial structure [14,21–25]. Despite these advantages for the design of model catalysts, in order to carry out fundamental investigations on catalytic mechanisms, studies of structural–activity relationship are still rarely found [26,27].

Furthermore, it shall be noticed that crystalline defects present on MOF-5 and ZIF-8 (zeolite imidazolate frameworks) are likely responsible for catalyzing some acid–base reactions [14,28]. Concerning ZIF-8, Chizallet et al. have reported its outstanding catalytic activity in transesterification reaction of vegetable oil with various alcohols [29]. From experimental and molecular modeling results, they have found that Zn(II) and Zn(III) species, which are Lewis acid sites, are located at the external surface and/or are bulk defects of ZIF-8. Moreover, the N^{-} at the extremity of monocoordinated imidazolate ligands as well as NH groups can participate as Brønsted bases.

On the other hand, water poisoning is an often encountered issue in catalysis [30–32]. Indeed, catalytic reactions can be hindered or just limited due to poisoning effects originating from moisture in the air or from the water formed as the product of reaction. Water molecules are irreversibly adsorbed on the catalytic sites, leading to catalyst deactivation. This motivates the design and engineering of catalytic materials with hydrophobic features – such as the hydrophobic outer shell of enzymes – in order to prevent water-induced catalyst poisoning. Cohen has reported hydrophobization of amino-containing MOF powders by post-synthetic modification, through amide coupling, using alkyl anhydrides [33]. In his study, the best results are obtained with an alkyl chain of 6 carbons and a minimum PSM yield of 17% to create a superhydrophobic MOF.

* Corresponding author.
E-mail address: david.farrusseng@ircelyon.univ-lyon1.fr (D. Farrusseng).

0021-9517/$ - see front matter © 2011 Elsevier Inc. All rights reserved.
doi:10.1016/j.jcat.2011.10.002

A key challenge for industrial use of MOFs is to deliver them in a shape suitable for applications [34,35]. Superhydrophobic properties of thin films used against biofouling are originated from a combined engineering at molecular level (low-surface-energy coatings such as perfluorinated compounds) and at macroscopic levels (rough surfaces) [36]. These studies are mainly based on nonporous materials, like silica wafers [37], polymer coatings [38,39] and metals [40–43]. Very few studies report superhydrophobic properties of microporous films [44].

Our team have already reported post-synthetic modification of a porous substituted imidazolate material, SIM-1. It belongs to the class of ZIF materials [45]. Zinc imidazolate SIM-1 is isostructural to ZIF-8 (SOD), which is commercialized under the name Basolite Z-1200 [46,47]. SIM-1 solid consists of $Zn–N_4$ tetrahedra linked by carboxyimidazolates. We have already reported that creating a hydrophobic environment by post-synthetic modification on SIM-1 powder can enhance the catalytic activity by an order of magnitude factor [48]. We have also described earlier the preparation of supported thin films of SIM on different alumina supports [49–53].

In this work, we report for the first time a quantitative structure–activity relationship of a functionalized MOF. Hydrophilic–hydrophobic balance of SIM, which drives the adsorption of water, is controlled by functionalization of the material by grafting C_{12} alkyl chains onto the framework. Surface tension properties are monitored by measuring the contact angle with a water droplet on SIM thin film grown on a flat support. We show that the contact angle is directly correlated to the catalytic activity of Knoevenagel condensation. Hence, we propose that the contact angle of a catalyst thin layer with water can be a quantitative descriptor of direct relevance for catalytic processes which produces water and/or for catalysts that are poisoned by water. We provide general principles and methodologies that can be applied to other type of porous materials such as zeolites or ordered mesoporous materials. Finally, we measured the intrinsic reaction rate free of external and internal diffusion limitations by controlling the thickness of SIM shell on SIM/alumina beads. Insights on the localization of the active sites (surface vs. bulk) are provided.

2. Materials and methods

2.1. Film preparation and characterization

All reactions are carried out in anhydrous solvents as received. All other reagents were commercially available and were used without further purification.

Hydrophobic features are quantified by measuring the contact angle of a water drop deposited on the dry material surface. For this measurement, supported SIM-1 thin films on flat alumina disks are synthesized following a general method already reported [51,53]. We used symmetric anodic alumina disks (13 mm diameter, 60 μm thickness, pore size 200 nm, supplied by Whatman, Fig. 1). The disk is immersed into a solution of $Zn(NO_3)_2{\cdot}4H_2O$ (0136 M) and 4-methyl-5-imidazolecarboxaldehyde (0,55 M). After a solvothermal treatment at 358 K for 48 h, the resulting supported material is washed with ethanol to remove the unreacted precursors and the fine SIM-1 unsupported particles. Supported SIM-1 on disk is then dried at room temperature.

Catalytic tests are carried out on eggshell type catalysts. Alumina beads are coated with SIM-1 layer following the synthesis procedure described above. Beads are α-alumina beads (1.5 mm diameter, BET area 2 $m^2\ g^{-1}$, supplied by Saint-Gobain Norpro, Fig. 1). In order to control the thickness of the films in SIM-1/α-alumina beads composites, synthesis time varies between 8, 24 and 48 h.

Thickness and homogeneity of SIM-1 films on α-alumina beads are characterized by SEM using a JSM 5800LV (JEOL). Tension range is 0.3–30 kV, and effective resolution is 0.5 nm at 30 kV.

Characterization of hydrophobic surfaces is usually performed by contact angle measurement with water. When the apparent water contact angle is lower than 90°, the surface is hydrophilic; when it is higher than 90°, the surface is hydrophobic; and when the contact angle is higher than 150°, the surface is coined as superhydrophobic [36]. Thus, hydrophobic properties of SIM materials are determined from contact angle of a water drop with SIM thin film on anodic alumina disk, a flat support being required. In practice, a drop of deionized water is deposited using a syringe on the surface of the sample, and the contact angle is determined from pictures made using a CCD camera [54]. The values are an average of three independent experiments.

Structure integrity of SIM layers is checked by Powder X-ray Diffraction (PXRD) directly on SIM/alumina flat disk or by crushing the SIM/alumina beads into fine powder with a mortar, and the data are collected at room temperature using a Bruker D5005 Diffractometer equipped with a secondary graphite monochromator (Cu Kα radiation, wavelengths λ = 0.154178 nm) and a scintillation counter.

2.2. Post-synthetic modification (PSM) procedure

Post-synthetic modification procedure is applied on both SIM-1/flat disk layer and eggshell SIM-1. SIM-1/alumina composites (one disk or 20 beads) are immersed in a solution of 7 mL of anhy-

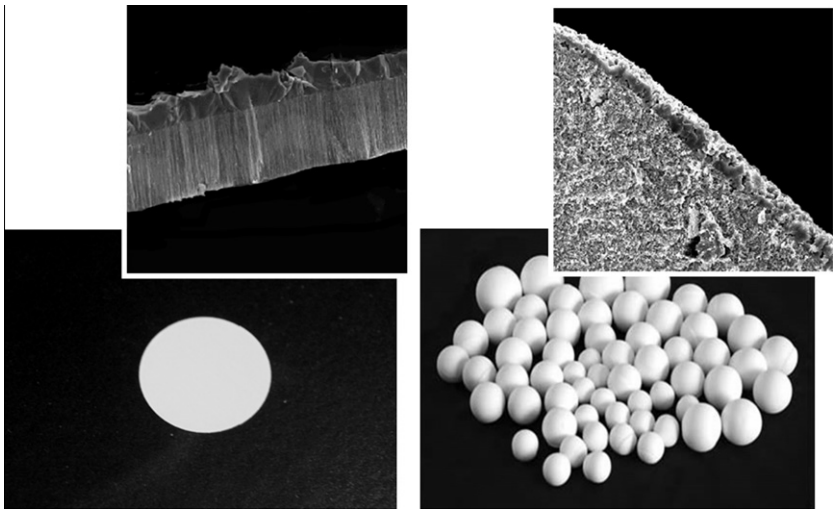

Fig. 1. Representative photographs of alumina supports, disk (left) and beads (right). Upper pictures show SIM/alumina cross-sections as observed by SEM.

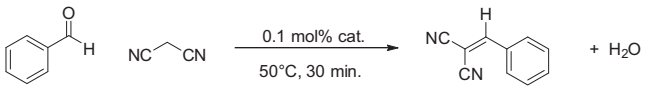

Scheme 1. Knoevenagel condensation catalyzed by SIMs.

drous methanol containing 390 mg of dodecylamine (2.1 mmol). The system is allowed to react at room temperature for the desired time without stirring. Then, the obtained SIM-2(C_{12})/alumina composite is washed three times with dry ethanol and dried at ambient temperature. Post-synthetic modification yield is adjusted by variation of reaction time. It corresponds to the conversion of aldehyde groups present in the SIM-1 structure. For example, a post-synthetic modification yield of 50% would correspond to the grafting of dodecylimino groups on half of the formyl moieties. Post-synthetic modification yield is determined by liquid ^{1}H NMR of a sample dissolved in a DCl/D_2O/dmso-d6 solution. For a typical preparation of an NMR tube, SIM composite is immersed in a minimum of the acidic deuterated solution and shaken by hand until a slight coloration of the solution showing dissolution of the SIM material. Solution is then separated from the alumina support and used for NMR analysis.

After the post-synthetic modification on flat alumina support, contact angles are measured, as described in Section 2.1, followed by NMR analysis. On the other hand, eggshell SIM-2(C_{12}) beads are used in Knoevenagel condensation.

2.3. Knoevenagel condensation

Knoevenagel reaction is a cross-aldol condensation between an aldehyde and an active methylene compound, which produces water as a side product (Scheme 1). This reaction is usually catalyzed by bases in solution or by some solids such as metal oxides [55].

In a typical catalytic run, 20 beads of SIM-2/alumina (c.a. 0.02 mmol of SIM-2(C_{12})) are introduced into a 10-mL glass vial. Benzaldehyde (20 mmol; 2 mL) and malononitrile (20 mmol; 1.32 g) are added, and the vial is sealed. The suspension is allowed to react at 323 K for 30 min. After quenching by cooling to 0 °C, the suspension is diluted (and the product dissolved) with Et_2O and the solid catalyst removed. The solution is then analyzed by gas chromatography and the yield determined by integration of signals using dodecane as an internal standard. In all cases, the turnover frequency (TOF) is calculated in this study as the catalytic yield after 30 min of reaction divided by the number of mol of SIM material (typically 0.02 mmol as indicated above) and by divided the reaction time. Blank experiments with bare alumina beads did not show significant activity [50].

3. Results

3.1. Hydrophobization of SIM-1/alumina composites by post-synthetic modification

Degree of functionalization, i.e., post-synthetic modification yield, is controlled by the reaction time between SIM-1 solid and dodecylamine, having a C_{12} aliphatic linear chain, without the use of catalyst or other agents (Scheme 2).

As expected, the longer time of reaction is, the higher is the yield of post-synthetic modification. By varying the reaction time from 8 to 48 h, post-synthetic modification yields vary from 1.5% to 6% for the flat disks. Complete dissolution of SIM layer by digestion in acidic DCl-D_2O-DMSO-d6 solution allows the exact quantification of functionalization by liquid ^{1}H NMR analysis. Presence in the NMR spectra of a new typical peak at 8.19 ppm, corresponding to the imino proton, confirms the efficiency of the organic transformation (Fig. 2). The proton of the imidazolyl is in turn shifted from

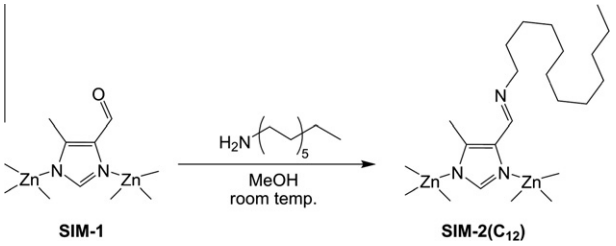

Scheme 2. Post-synthetic modification of SIM-1 with dodecylamine to give SIM-2(C_{12}).

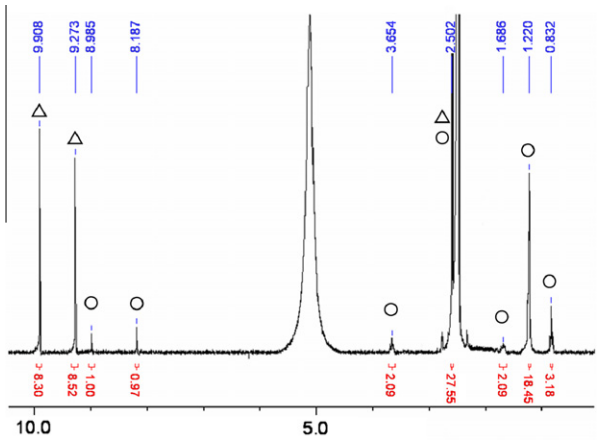

Fig. 2. Liquid ^{1}H NMR of digested SIM-2(C_{12})/alumina samples. Unmodified linker of SIM-1 and functionalized SIM-2(C_{12}) is indicated by triangles and circles, respectively.

9.27 to 8.98 ppm. Moreover, no remaining free dodecylamine is detected between 0.5 and 4 ppm.

The yield is determined by integration of the NMR signals and is obtained by taking the ratio between those of SIM-2(C_{12}) normalized to 1 and those of SIM-1 in the aromatic range (Fig. 3).

Moreover, structural integrity of the material is preserved throughout the film growth and the post-synthetic modification according to the PXRD analysis (Fig. 4).

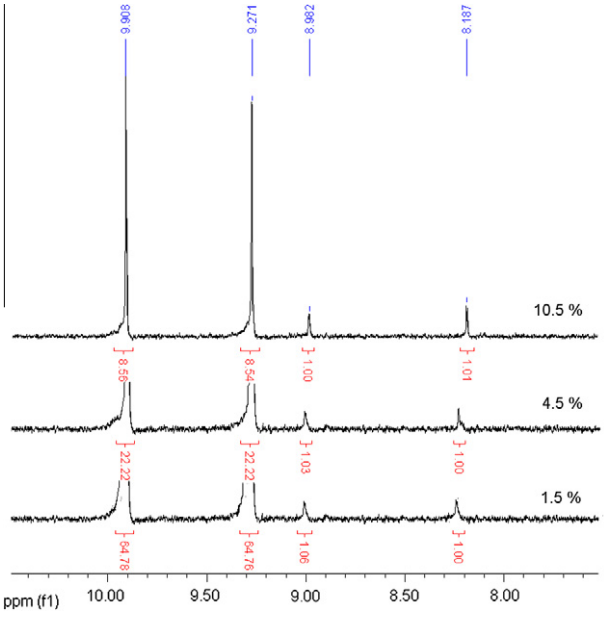

Fig. 3. Quantification of post-synthetic modification yield by liquid ^{1}H NMR analysis of three SIM-2(C_{12}) eggshell composites.

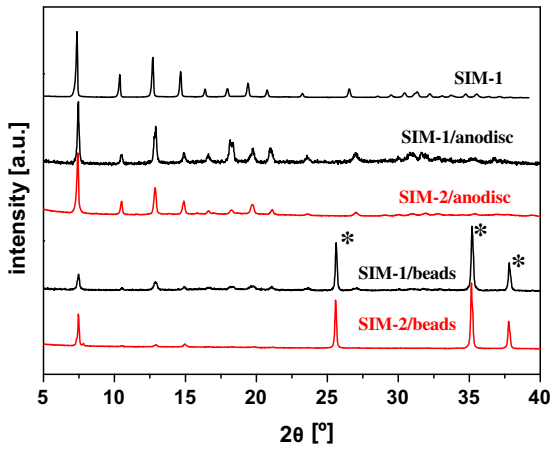

Fig. 4. PXRD patterns of as-synthesized and supported SIM-1 or SIM-2(C_{12}) on alumina disks and beads. Reflections marked by * correspond to α-alumina.

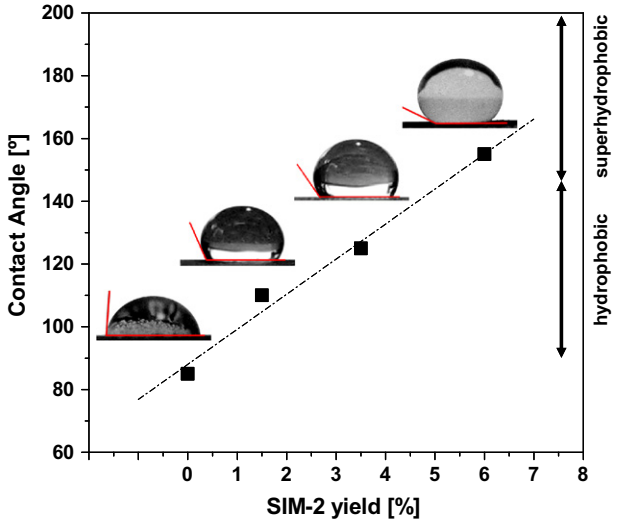

Fig. 5. Evolution of the contact angle water drop/SIM-2(C_{12}) layer with the post-functionalization yield.

Hydrophobicity of SIM thin films on flat alumina disks is quantified by the contact angle of water with the surface. Influence of the post-functionalization yield on the contact angle is shown in Fig. 5. Interestingly, we can observe a linear correlation between post-synthetic modification yield and the contact angle. SIM-1 film (0% of post-synthetic modification) presents a minimum water contact angle of 85°, showing that SIM-1 is at the boundary between hydrophilic and hydrophobic material. When yields of functionalization increase up to 1.5% and 3.5%, the water contact angles reach 110° and 125°, respectively. This range of contact angle is typical for hydrophobic surfaces. Furthermore, a contact angle of 155° is found when the post-synthetic modification yield is 6%, leading to a superhydrophobic surface. In the last sample, the water droplet can easily roll off the surface. As a result, we can observe that minor to modest post-synthetic modification yields have a strong impact on the surface tension of the surface, the surface passing from hydrophilic to superhydrophobic.

Following a similar strategy, SIM-1 eggshell composites (beads) are involved in the same post-synthetic modification procedure. By variation of the reaction time from 2 to 48 h, the degree of functionalization of SIM-2(C_{12})/beads composites is adjusted to reach yields from 1.5% to 10.5%, as determined by NMR. According to the results obtained with disks and the correlation between the post-synthetic modification yield and the hydrophobic behavior, C_{12} aliphatic chains present in the material are supposed to create a hydrophobic environment in the SIM-2(C_{12}) layer on beads (Fig. 6).

3.2. Knoevenagel condensation using eggshell SIM/alumina beads

We perform the Knoevenagel reaction under solvent-free conditions at 50 °C, using SIM-2(C_{12})/alumina beads composites with different post-synthetic modification yields as catalysts. In order to maintain the integrity of the SIM film attached to the alumina beads while stirring the substrates solution (800 rpm), catalytic tests are performed using a tea-bag system allowing the immersion of the beads into the catalytic solution and avoiding attrition issues. Fig. 7 clearly shows a linear increase in the catalytic activity of SIM-2(C_{12})/alumina eggshell catalysts with post-synthetic modification yield, which represents an increasing amount of grafted C_{12} chains. SIM-2(C_{12}) on alumina beads shows a TOF = 1500 h^{-1} for a degree of modification of 10.5% when the equivalent SIM-1 beads show a TOF = 215 h^{-1}; it corresponds to a 7-fold increase. In order to investigate whether dissolved species might be the catalytic species, leaching tests are performed. After removing the tea bag containing the beads while the solution is stirred under catalytic conditions, no further reaction takes place. In addition, catalytic activity of pure dodecylamine, having similar basicity than the corresponding imines, is measured under the same conditions leading to a TOF = 450 h^{-1}. Catalytic activity of SIM-2(C_{12}) can therefore not be explained by the combination of activities of both SIM-1 basic species and dodecylamine.

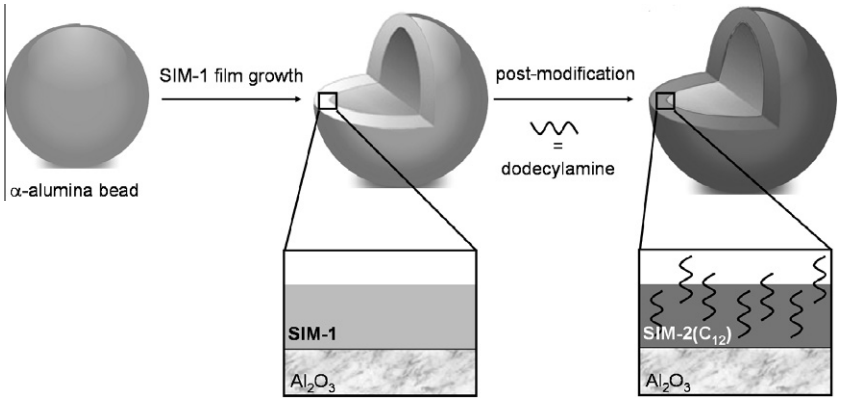

Fig. 6. Post-synthetic hydrophobization of α-Al_2O_3 bead-supported SIM material.

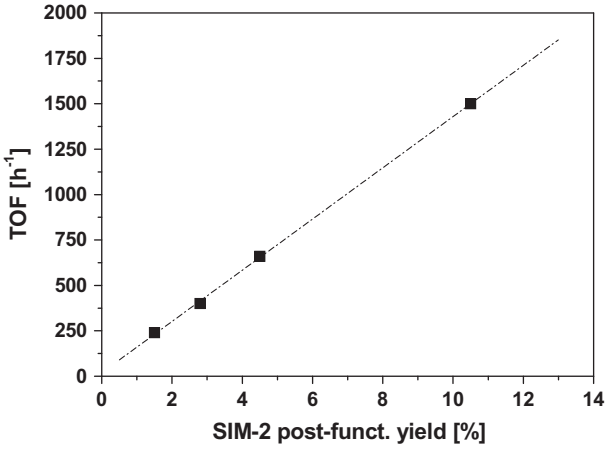

Fig. 7. Evolution of the catalytic activity with post-functionalization yield on SIM-2/α-alumina beads for Knoevenagel condensation.

Location of the active sites (surface or core) as well as the study of diffusion limitation can be determined under fine control of the thickness of the SIM-1 shell. We have varied synthesis time between 8, 24 and 48 h to get different thickness of the layer. The thickness of the SIM-1 shell on alumina beads is measured by SEM. Cross-section pictures are taken by slicing through the samples. Fig. 8 shows the morphology of bead-supported SIM-1/Al_2O_3. It shows average layer thicknesses of 1.3, 4 and 10 μm corresponding to the synthesis times of 8, 24 and 48 h, respectively. On the bottom part, a lower magnification of SEM pictures shows a good homogeneity of the film along the surface of the alumina beads. We did not observe measurable amounts of Zn by EDX in the core of the bead, suggesting that SIM-1 is only present at the surface of the bead [49].

Catalytic tests are performed using a constant number of beads (c.a. 10 SIM-1/alumina beads). Considering the diameter of the alumina beads and the layer thickness, the SIM-1 external surface on the three types of composites (Fig. 8) can be considered as constant when the amount of SIM-1 is increasing with increasing film thickness. Indeed, the diameter of the alumina beads used is 1.5 mm, and the thickness of the SIM-1 layer varies from 1.3 to 10 μm. According to the formula giving the area of a sphere, the external surface of the SIM-1/alumina bead composites varies from 7.093 to 7.258 mm^2. Thus, by increasing the thickness of the SIM-1 layer by almost 8 times, the external accessible surface of SIM-1 increases by 2%. We consequently assume that the external SIM-1 surface is kept constant whatever the SIM-1/alumina bead composite used.

Interestingly, the yield plot clearly shows that the Knoevenagel reaction yield is increasing almost linearly with the layer thickness of the SIM-1 beads (Fig. 9). In agreement, we can observe that the TOF, taking into account both the catalytic yield and the quantity of SIM-1 catalyst used, is constant whatever the thickness involved. According to these results, the catalytic activity strongly depends on the quantity of the SIM-1 catalyst and not on the amount of its surface area. We can thus assume that there is a catalytic contribution of the SIM material throughout the whole layer and not only from the surface species. For unsupported SIM-1 catalyst and for the eggshell SIM-1/alumina, the TOF values fall in the same range, 180 s^{-1} and 220 s^{-1} for the powder and for the eggshell, respectively. Hence, similar TOFs are obtained, whereas the particle diameter differs by three orders of magnitude. Therefore, we can conclude that the reaction is not limited by external diffusion in the tea bag. In addition, we can observe that TOF is constant whatever the thickness involved. According to these results, the catalytic activity is not internal diffusion limited. We can thus assume that there is a catalytic contribution of the SIM material throughout the whole layer and not only from surface species.

4. Discussion

4.1. Degree of functionalization

In a previous study, Caro and Huang already used supported ZIF-90 on a ceramic tube to perform post-synthetic modification in order to enhance hydrogen selectivity but without evaluating the functionalization yield [56]. Yaghi et al. also reported functionalization of porous materials as powder [57] and especially the reactivity of ZIF-90 toward an amine or a reducing agent [58]. Post-synthetic modification described in the latter is complete (100%). However, in the case of an incomplete functionalization,

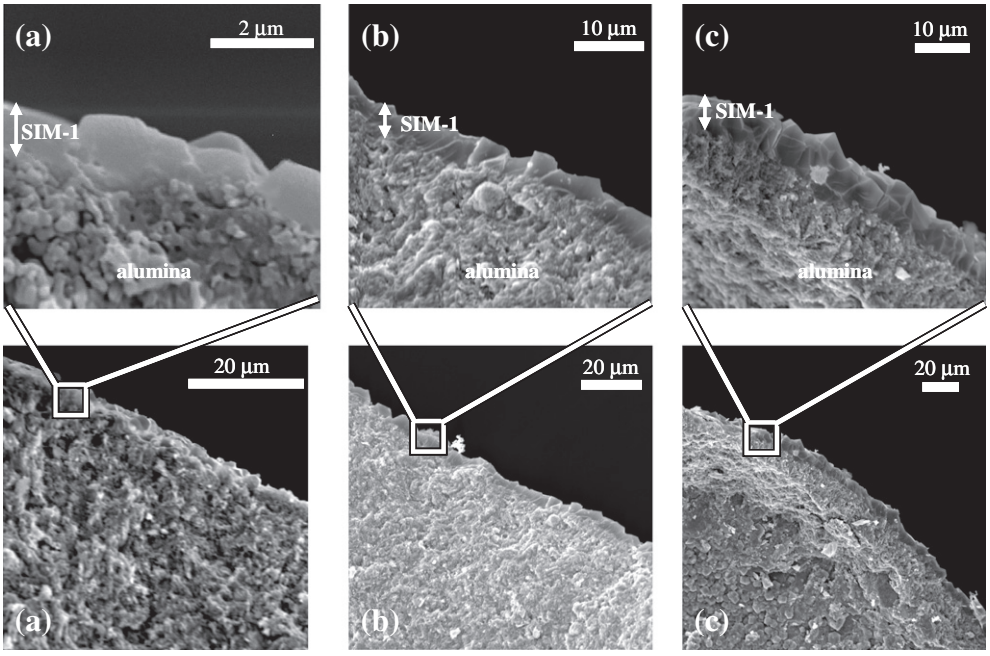

Fig. 8. SIM-1 supported on α-alumina beads with synthesis time of 8 h (a), 24 h (b) and 48 h (c).

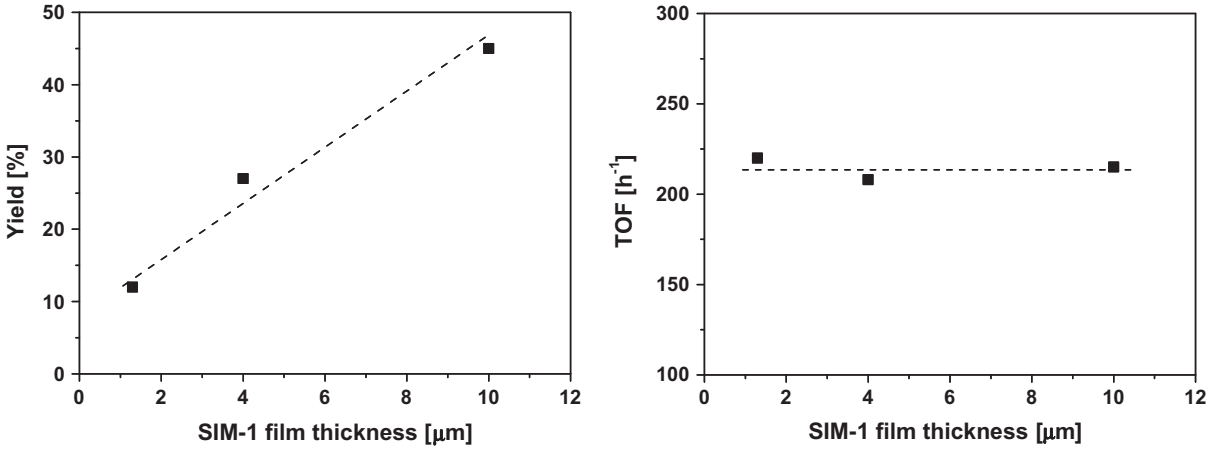

Fig. 9. Evolution of the yield (left) and the TOF (right) of the Knoevenagel condensation vs. the thickness of the SIM-1 layer.

where less than 100% of the functional groups are modified, homogeneity of the modification throughout the whole material should be discussed.

In this study, PSM yields are comprised between 1% and 11% as determined by NMR. Such yields could not be obtained if only the formyl moieties available at the external surface of the layer would have reacted. Indeed, the surface atomic layer corresponds only to 1 nm, whereas the crystal thickness ranges from 1 to 10 μm (3–4 orders of magnitude larger). Hence, the post-functionalization mainly occurs in the porosity of the SIM layers, even if a gradient of functionalization, decreasing from the surface to the core, cannot be excluded. This gradient, if any, would depend on the relative reaction rate and diffusion rate of the amines into the porous frameworks.

4.2. Contact angle on thin film as macroscopic descriptor of surface property for porous catalysts

Measurement of the contact angle using MOF thin film is a well appropriate technique to quantify the level of hydrophobicity. It is important to note that this technique cannot be applied, in principle, on dispersed powders since the contact angle depends on a solid–gas and liquid–gas interfaces. Hence, the size of the crystallites and their packing have a direct impact on the contact angle. As a matter of fact, measurement should be taken on flat surfaces in order to probe the surface tension of the solids.

As described above, we observe a linear relationship between post-synthetic modification yield of SIM-2(C_{12})/flat support and the contact angle (Fig. 5). We can suppose that this linear relationship also exists on the eggshell SIM/alumina composites. Moreover, Fig. 7 shows a linear relation between post-synthetic modification yield of SIM-2(C_{12})/beads and their catalytic activities in Knoevenagel reaction. By extrapolation of the contact angle for post-synthetic modification yields reaching 10%, we build a plot representing the catalytic activity (TOF) as a function of the calculated contact angle, used as a descriptor of the hydrophobicity (Fig. 10).

From this plot, we can clearly see that a minimum level of hydrophobicity is required in order to accelerate the reaction until a maximum superhydrophobicity is reached.

The hydrophilic–hydrophobic balance of the catalytic MOFs is usually not or poorly characterized, although it may drive co-adsorption competition of the various reactants or products of the reactions. Characterization can be carried out by measuring the adsorption of each reactant or product individually by gravimetric or volumetric methods. However, it is often tedious and time consuming. We believe that this methodology could be applied more generally on other catalytic systems such as oxides or carbons as long as thin layers with low roughness can be prepared. In this approach, the contact angle is a macroscopic indicator of the surface tension which arises from the surface composition at molecular scale.

4.3. Upgrading by modification of the environment/ adsorption properties

The aforementioned variable hydrophobization of SIM surface through its functionalization with dodecylimino groups and these catalytic results tend to confirm that hydrophobic chains anchored into the solid, in the vicinity of the catalytic centers, limit adsorption or favor desorption of water molecules and make these centers free to adsorb the substrates. We can thus attribute the significant acceleration of the reaction rate to the modification of the environment of the catalytic sites.

There is a large amount of water produced during the reaction, corresponding to 2–15 mmol of water depending on the reaction yield. From N_2 isotherm, the porous volume of SIM-1 is 0.2 $cm^3\ g^{-1}$, which is the accessible volume inside SIM-1 [49]. This means that to fill 0.02 mmol of SIM-1 (used for a catalytic run), it would require 0.05 mmol of H_2O. Besides, from H_2O isotherms, we showed that 0.02 mmol of SIM-1 experimentally adsorbs a maximum quantity of 0.046 mmol of H_2O [48]. Taking into account the amount of SIM material (about 0.02 mmol) involved, we can assume that, in the case of SIM-2(C_{12}), water is not trapped into

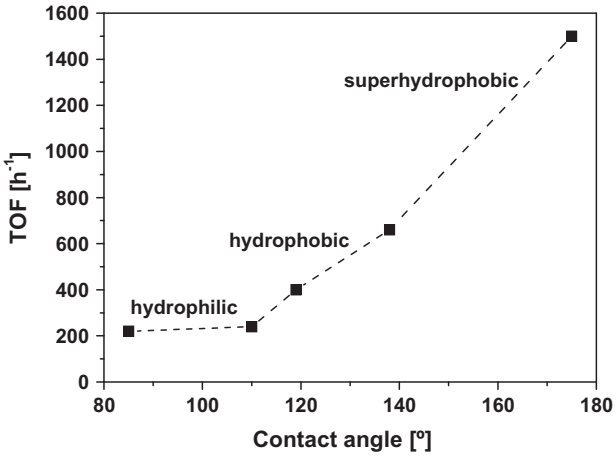

Fig. 10. Correlation between catalytic activities and extrapolated contact angles.

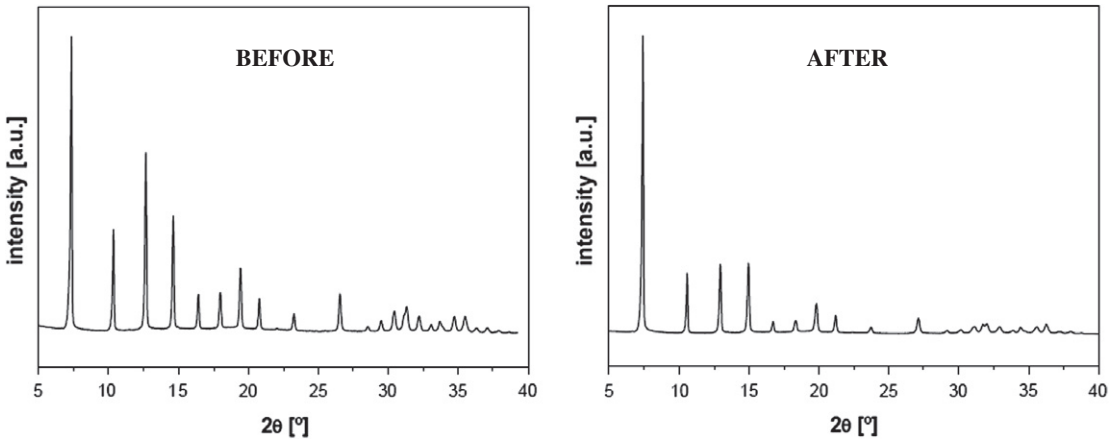

Fig. 11. PXRD patterns of SIM-1 before and after treatment in boiling water for 24 h.

the porous layer but is instead evacuated to the solution. Besides, the stability of ZIF materials is already reported [59–61], and crystallinity of SIM-1 remains intact after treatment in boiling water (Fig. 11).

Fine control of the post-synthetic modification yield allows tuning hydrophobic properties from hydrophilic to hydrophobic and even superhydrophobic, leading to improved catalytic activities for a water-producing reaction. As already mentioned, Knoevenagel condensation has been found to be catalyzed by basic solids and especially by MOFs such as MIL-101, IRMOF-3 or MIL-53, having basic sites in their as-synthesized form or being modified in order to anchor active moieties [15,62,63]. They, however, show turnover frequencies up to 330 h^{-1}, ten times lower than those obtained under similar conditions with the superhydrophobic SIM-2(C_{12}). In this study, our strategy is not based on the introduction of new catalytic sites but on the creation of a hydrophobic environment surrounding those existing sites. Corma et al. already reported similar conclusions on a hydrophobic Ti-MCM-41 used as catalyst for epoxidation reaction [64]. Hydrophobic features of this mesoporous silica are influencing its catalytic activity by avoiding deactivation from water contained in the substrates and from diol side product formed during a parallel reaction of the epoxide with water.

4.4. Nature and location of active sites

Using FTIR and DFT calculations, Chizallet et al. demonstrate that acido–basic sites of ZIF-8 are located at the external surface of the solids or at crystalline defects [29,65]. Possible basic sites could be nitrogen from imidazolate ring, which are monocoordinated. The strength and the number of this type of sites are yet unknown. In addition, Chizallet et al. have identified possible Lewis and Bronsted sites such as Zn–OH and N–H, respectively. Therefore, the exact nature and numbers of basic sites for SIM-1 have still to be investigated, but we can assume that there are similar to those of ZIF-8. On the other hand, when the post-modification is performed, imine groups are created which could potentially act as possible base centers. However, catalytic results suggest that it seems not to be the case. Under the same catalytic conditions, 0.02 mmol of SIM-1/beads shows a TOF of 215 h^{-1}, while 0.02 mmol of dodecylamine shows a TOF of 450 h^{-1}. After post-modification, the SIM-2(C12) possesses dodecylimino groups having the same basicity than the dodecylamine (pKa around 10). However, 0.02 mmol of SIM-2(C12)/beads, functionalized with 10.5% of imino group (c.a. 0.002 mmol of dodecylimino groups), shows a TOF of 1500 h^{-1}. The activity of SIM-2(C12) is thus three times higher than that of the dodecylamine, whereas ten times less of basic groups are introduced into the catalytic reaction. The catalytic performance of the SIM-2(C12) can thus not lie only in the presence of new imino basic groups, neither in their combination with basic sites already present in the parent SIM-1.

From this study, experiments performed using different SIM-1 layer thicknesses tend to prove that catalytic species could be found deep inside the material and not only at the surface. As found for ZIF-8, active species can be structural defects such as open zinc sites, hydroxyls or monocoordinated imidazolates but dispersed in the core of the material. This provides a new income in order to define the exact nature of active sites in ZIFs materials. In addition, aromatic hydrocarbons diffusivity in zeolite materials is found to be around 10^{-9} m^2 s^{-1} [66]. In the case of SIM-1, the estimated characteristic diffusion time is between 1.5×10^{-3} s (for a layer thickness of 10 μm) and 10^{-2} s (for a layer thickness of 1.5 μm) when the inverse of the TOF, corresponding to the characteristic reaction time, is 20 s. That means, it takes 2000 times longer for organic molecules to react together to give the Knoevenagel adduct than to pass through the whole SIM-1 layer, proving the absence of intragranular diffusion limitation. Furthermore, the SIM-2(C_{12}) powder (22% functionalized) with crystallite size of 200 nm shows a TOF of 1920 h^{-1} [48] when its bead-supported analog (10.5% functionalized) with a bead diameter of 1.5 mm shows a TOF of 1500 h^{-1}. Based on the absence of catalytic species leaching in the both cases, we can assume that there is no extragranular diffusion limitation.

5. Conclusions

We have shown upgrading of a supported metal-organic framework catalyst through its post-synthetic functionalization. Keeping the catalytic center the same, post-synthetic modification enables an efficient control of the hydrophilic–hydrophobic balance that drives the competitive adsorption of reactants and products. Hence, we attribute the increase in the reaction rate of Knoevenagel condensation (up to seven times) to modification of the environment of catalytic sites through the creation of hydrophobic environment surrounding catalytic sites, as found in enzymes.

We have shown that the contact angle of catalytic surfaces with water is a relevant feature for describing the activity of the Knoevenagel condensation, assuming that the basicity is not significantly changed. It appears that a minimum level of hydrophobicity is required to observe an increase in the activity while superhydrophobic materials are very active. Hence, we propose that the contact angle that is a physicochemical measure at macroscopic scale could be a

relevant descriptor of the adsorption properties of porous solids which drive their catalytic properties at the molecular scale. We believe that this methodology could be applied for other porous materials such as aluminosilicates and carbon-based materials.

Acknowledgment

The authors are very grateful to IRCELYON scientific services.

References

[1] A. Corma, H. Garcia, F.X.L. Xamena, Chem. Rev. 110 (2010) 4606–4655.
[2] D. Farrusseng, S. Aguado, C. Pinel, Angew. Chem., Int. Ed. 48 (2009) 7502–7513.
[3] G. Ferey, Chem. Soc. Rev. 37 (2008) 191–214.
[4] S.T. Meek, J.A. Greathouse, M.D. Allendorf, Adv. Mater. 23 (2011) 249–267.
[5] O. Shekhah, J. Liu, R.A. Fischer, C. Woell, Chem. Soc. Rev. 40 (2011) 1081–1106.
[6] G. Nickerl, A. Henschel, R. Grunker, K. Gedrich, S. Kaskel, Chem. Ing. Technol. 83 (2011) 90–103.
[7] C. Wang, Z. Xie, K.E. Dekrafft, W. Lin, J. Am. Chem. Soc. 133 (2011) 13445–13454.
[8] L.H. Wee, L. Alaerts, J.A. Martens, D. De Vos, Metal-organic frameworks as catalysts for organic reactions, in: Metal-Organic Frameworks, Wiley-VCH Verlag GmbH & Co. KGaA, 2011, pp. 191–212.
[9] L. Alaerts, Chem. Eur. J. 12 (2006) 7353–7363.
[10] P. Horcajada, S. Surble, C. Serre, D.Y. Hong, Y.K. Seo, J.S. Chang, J.M. Greneche, I. Margiolaki, G. Ferey, Chem. Commun. (2007) 2820–2822.
[11] K. Schlichte, T. Kratzke, S. Kaskel, Micropor. Mesopor. Mater. 73 (2004) 81–88.
[12] K.K. Tanabe, S.M. Cohen, Angew. Chem., Int. Ed. 48 (2009) 7424–7427.
[13] F. Xamena, A. Abad, A. Corma, H. Garcia, J. Catal. 250 (2007) 294–298.
[14] U. Ravon, M. Savonnet, S. Aguado, M.E. Domine, E. Janneau, D. Farrusseng, Micropor. Mesopor. Mater. 129 (2010) 319–329.
[15] Y.K. Hwang, D.Y. Hong, J.S. Chang, S.H. Jhung, Y.K. Seo, J. Kim, A. Vimont, M. Daturi, C. Serre, G. Ferey, Angew. Chem., Int. Ed. 47 (2008) 4144–4148.
[16] J.S. Seo, D. Whang, H. Lee, S.I. Jun, J. Oh, Y.J. Jeon, K. Kim, Nature 404 (2000) 982–986.
[17] G. Ferey, C. Serre, Chem. Soc. Rev. 38 (2009) 1380–1399.
[18] S.M. Cohen, Chem. Sci. 1 (2010) 32–36.
[19] K.K. Tanabe, S.M. Cohen, Chem. Soc. Rev. 40 (2011) 498–519.
[20] Z.Q. Wang, S.M. Cohen, Chem. Soc. Rev. 38 (2009) 1315–1329.
[21] S. Chavan, J.G. Vitillo, M.J. Uddin, F. Bonino, C. Lamberti, E. Groppo, K.P. Lillerud, S. Bordiga, Chem. Mater. 22 (2010) 4602–4611.
[22] X.-Y. Cui, Z.-Y. Gu, D.-Q. Jiang, Y. Li, H.-F. Wang, X.-P. Yan, Anal. Chem. 81 (2009) 9771–9777.
[23] M.J. Ingleson, J.P. Barrio, J.B. Guilbaud, Y.Z. Khimyak, M.J. Rosseinsky, Chem. Commun. (2008) 2680–2682.
[24] M. Savonnet, D. Bazer-Bachi, N. Bats, J. Perez-Pellitero, E. Jeanneau, V. Lecocq, C. Pinel, D. Farrusseng, J. Am. Chem. Soc. 132 (2010) 4518–4519.
[25] X. Zhang, F. Llabres, A. Corma, J. Catal. 265 (2009) 155–160.
[26] L.Q. Ma, J.M. Falkowski, C. Abney, W.B. Lin, Nat. Chem. 2 (2010) 838–846.
[27] F. Song, C. Wang, J.M. Falkowski, L. Ma, W. Lin, J. Am. Chem. Soc. 132 (2010) 15390–15398.
[28] M. Savonnet, S. Aguado, U. Ravon, D. Bazer-Bachi, V. Lecocq, N. Bats, C. Pinel, D. Farrusseng, Green Chem. 11 (2009) 1729–1732.
[29] C. Chizallet, S. Lazare, D. Bazer-Bachi, F. Bonnier, V. Lecocq, E. Soyer, A.A. Quoineaud, N. Bats, J. Am. Chem. Soc. 132 (2010) 12365–12377.
[30] G. Di Carlo, G. Melaet, N. Kruse, L.F. Liotta, G. Pantaleo, A.M. Venezia, Chem. Commun. 46 (2010) 6317–6319.
[31] J.Y. Park, Z.M. Wang, D.K. Kim, J.S. Lee, Renew. Energy 35 (2010) 614–618.
[32] H.Y. Wang, W.F. Schneider, Surf. Sci. 603 (2009) L91–L94.
[33] J.G. Nguyen, S.M. Cohen, J. Am. Chem. Soc. 132 (2010) 4560–4561.
[34] P. Küsgens, A. Zgaverdea, H.-G. Fritz, S. Siegle, S. Kaskel, J. Am. Ceram. Soc. 93 (2010) 2476–2479.
[35] E.V. Ramos-Fernandez, M. Garcia-Domingos, J. Juan-Alcañiz, J. Gascon, F. Kapteijn, Appl. Catal., A 391 (2010) 261–267.
[36] X. Zhang, F. Shi, J. Niu, Y.G. Jiang, Z.Q. Wang, J. Mater. Chem. 18 (2008) 621–633.
[37] J.L. Lou, H.W. Shiu, L.Y. Chang, C.P. Wu, Y.L. Soo, C.H. Chen, Langmuir 27 (2011) 3436–3441.
[38] T. Pisuchpen, N. Chaim-Ngoen, N. Intasanta, P. Supaphol, V.P. Hoven, Langmuir 27 (2011) 3654–3661.
[39] Y.T. Tsai, C.H. Choi, N. Gao, E.H. Yang, Langmuir 27 (2011) 4249–4256.
[40] M.K. Dawood, H. Zheng, T.H. Liew, K.C. Leong, Y.L. Foo, R. Rajagopalan, S.A. Khan, W.K. Choi, Langmuir 27 (2011) 4126–4133.
[41] R.G. Karunakaran, C.H. Lu, Z.H. Zhang, S. Yang, Langmuir 27 (2011) 4594–4602.
[42] K.R. Khedir, G.K. Kannarpady, H. Ishihara, J. Woo, C. Ryerson, A.S. Biris, Langmuir 27 (2011) 4661–4668.
[43] X.D. Zhao, H.M. Fan, X.Y. Liu, H.H. Pan, H.Y. Xu, Langmuir 27 (2011) 3224–3228.
[44] A.V. Rao, A.B. Gurav, S.L.A. Sanjay, R.S. Vhatkar, H. Imai, C. Kappenstein, P.B. Wagh, S.C. Gupta, J. Colloid Interf. Sci. 352 (2010) 30–35.
[45] Y. Liu, V.C. Kravtsov, R. Larsen, M. Eddaoudi, Chem. Commun. 14 (2006) 1488–1490.
[46] X. Huang, Y. Lin, J. Zhang, X. Chen, Angew. Chem., Int. Ed. 45 (2006) 1557–1559.
[47] X. Huang, J. Zhang, X. Chen, Chin. Sci. Bull. 48 (2003) 1531–1534.
[48] J. Canivet, S. Aguado, C. Daniel, D. Farrusseng, ChemCatChem 3 (2011) 675–678.
[49] S. Aguado, J. Canivet, D. Farrusseng, Chem. Commun. 46 (2010) 7999–8001.
[50] S. Aguado, J. Canivet, D. Farrusseng, J. Mater. Chem. 21 (2011) 7582–7588.
[51] S. Aguado, C.H. Nicolas, V. Moizan-Baslé, C. Nieto, H. Amrouche, N. Bats, N. Audebrand, D. Farrusseng, New J. Chem. 35 (2011) 41–44.
[52] D. Farrusseng, S. Aguado, J. Canivet, WO Patent 2011033233, 2009.
[53] D. Farrusseng, S. Aguado, C.H. Nicolas, B. Siret, S. Durecu, WO Patent 2011033235, 2009.
[54] N.A. Patankar, Langmuir 19 (2003) 1249–1253.
[55] A. Corma, S. Iborra, Optimization of alkaline earth metal oxide and hydroxide catalysts for base-catalyzed reactions, in: Adv. Catal., 2006, pp. 239–302.
[56] A. Huang, J. Caro, Angew. Chem., Int. Ed. 50 (2011) 4979–4982.
[57] C.J. Doonan, W. Morris, H. Furukawa, O.M. Yaghi, J. Am. Chem. Soc. 131 (2009) 9492–9493.
[58] W. Morris, C.J. Doonan, H. Furukawa, R. Banerjee, O.M. Yaghi, J. Am. Chem. Soc. 130 (2008) 12626–12627.
[59] R. Banerjee, H. Furukawa, D. Britt, C. Knobler, M. O'Keeffe, O.M. Yaghi, J. Am. Chem. Soc. 131 (2009) 3875.
[60] R. Banerjee, A. Phan, B. Wang, C. Knobler, H. Furukawa, M. O'Keeffe, O.M. Yaghi, Science 319 (2008) 939.
[61] J.J. Low, A.I. Benin, P. Jakubczak, J.F. Abrahamian, S.A. Faheem, R.R. Willis, J. Am. Chem. Soc. 131 (2009) 15834–15842.
[62] J. Gascon, U. Aktay, M.D. Hernandez-Alonso, G.P.M. van Klink, F. Kapteijn, J. Catal. 261 (2009) 75–87.
[63] J. Juan-Alcaniz, E.V. Ramos-Fernandez, U. Lafont, J. Gascon, F. Kapteijn, J. Catal. 269 (2010) 229–241.
[64] A. Corma, M. Domine, J.A. Gaona, J.L. Jorda, M.T. Navarro, F. Rey, J. Perez-Pariente, J. Tsuji, B. McCulloch, L.T. Nemeth, Chem. Commun. (1998) 2211–2212.
[65] C. Chizallet, N. Bats, J. Phys. Chem. Lett. 1 (2010) 349–353.
[66] T. Masuda, Y. Fujikata, T. Nishida, K. Hashimoto, Micropor. Mesopor. Mater. 23 (1998) 157–167.